

1-Dimensional polynomial neural networks for audio signal related problems

Habib Ben Abdallah*, Christopher J. Henry, Sheela Ramanna

Department of Applied Computer Science, University of Winnipeg, Winnipeg, Manitoba, Canada

Abstract

In addition to being extremely non-linear, modern problems require millions if not billions of parameters to solve or at least to get a good approximation of the solution, and neural networks are known to assimilate that complexity by deepening and widening their topology in order to increase the level of non-linearity needed for a better approximation. However, compact topologies are always preferred to deeper ones as they offer the advantage of using less computational units and less parameters. This compacity comes at the price of reduced non-linearity and thus, of limited solution search space. We propose the 1-Dimensional Polynomial Neural Network (1DPNN) model that uses automatic polynomial kernel estimation for 1-Dimensional Convolutional Neural Networks (1DCNNs) and that introduces a high degree of non-linearity from the first layer which can compensate the need for deep and/or wide topologies. We show that this non-linearity introduces more computational complexity but enables the model to yield better results than a regular 1DCNN that has the same number of training parameters on various classification and regression problems related to audio signals. The experiments were conducted on three publicly available datasets and demonstrate that the proposed model can achieve a much faster convergence than a 1DCNN on the tackled regression problems.

Keywords: Audio signal processing, convolutional neural networks, denoising, machine learning, polynomial approximation, speech processing.

1. Introduction

The Artificial Neural Network (ANN) has nowadays become an extremely popular model for machine-learning applications that involve classification or regression [1]. Due to its effectiveness on feature-based problems, it has been extended with many variants such as Convolutional Neural Networks (CNNs) [2, 3] or Recurrent Neural Networks (RNNs) [4, 5] that aim to solve a broader panel of problems involving signal processing [6, 7] and/or time-series [8, 9] for example. However, as data is becoming more available to use and exploit, problems are becoming richer and more complex, and deeper and bigger topologies [10, 11] of neural networks are used to solve them. Moreover, the computational load to train such models is steadily increasing - despite advances in high performance computing systems - and it may take up to several days just to develop a trained model that generalizes well on a given problem. This aggravation is partially due to the fact that complex problems involve highly non-linear solution spaces, and, to achieve a high level of non-linearity, deeper topologies [12] are required since every network layer introduces a certain level of non-linearity with an activation function.

A well known machine-learning trick to alleviate such a problem is to resort to a *kernel transformation* [13, 14]. The basic idea is to apply a non-linear function (that has certain properties) to the input features so that the search space becomes slightly non-linear and maybe (not always) more adequate to solve the given

*Corresponding author.

Email addresses: benabdallah-h@webmail.uwinnipeg.ca (Habib Ben Abdallah), ch.henry@uwinnipeg.ca (Christopher J. Henry), s.ramanna@uwinnipeg.ca (Sheela Ramanna)

problem. However, such a trick highly depends on the choice of the so-called *kernel*, and may not be successful due to the fact that the non-linearity of a problem can not always be expressed through usual functions; e.g. polynomial, exponential, logarithmic or circular functions. Moreover, the search for an adequate kernel involves experimenting with different functions and evaluating their individual performance which is time consuming. One can also use the kernel trick with neural networks [15, 16] but the same problem remains: What is an adequate kernel for the given problem? The proposed model creates a variant of 1-Dimensional CNN (1DCNN) that can estimate kernels for each neuron using a polynomial approximation with a given degree for each layer. This work aims to demonstrate that the non-linearity introduced by polynomial approximation may help to reduce the depth (number of layers) or at least the width (number of neurons per layer) of the conventional neural network architectures due to the fact that the kernels estimated are dependent on the problems that are considered, and more specific than the well-known general kernels.

The contribution of this work is a novel variant of 1DCNN which we call 1-Dimensional Polynomial Neural Network (1DPNN) designed to create the adequate kernels for each neuron in an automated way, and thus, better approximate the non-linearity of the solution space by increasing the complexity of the search space. We present a formal definition of the 1DPNN model which includes forward and backward propagation, a new weight initialization method, and a detailed theoretical computational complexity analysis. Our proposed 1DPNN is evaluated in terms of the number of parameters, the computational complexity, and the estimation performance for various audio signal applications involving either classification or regression. Two classification problems were considered, musical note recognition on a subset of the NSynth[17] dataset and spoken digit recognition on the Free Spoken Digits dataset [18]. Identically, two regression problems were considered for which a subset of the MUSDB18 [19] dataset was used, namely audio signal denoising and vocal source separation. Our evaluation methodology is based on comparing the performance of the 1DPNN to that of the 1DCNN under certain conditions, notably, the equality of the number of trainable parameters. Therefore, we chose not to create very deep and wide networks and to restrict our analysis to a fairly manageable number of parameters due to technical limitations.

The outline of our paper is as follows. Section 2 discusses the major contributions made regarding the introduction of additional non-linearities in neural networks. Section 3 formulates the model mathematically by detailing how the forward propagation and the backward propagation are performed as well as providing new way to initialize the weights and a detailed theoretical computational analysis of the model while Section 4 describes how it was implemented and tackles the computational analysis from an experimental perspective. Section 5 describes in detail the experiments that were conducted in order to evaluate the model, and shows its results, and finally, Section 6 addresses the strengths and the weaknesses of the model and proposes different ways of extending and improving it.

2. Related Work

Many of the works that try to add a degree of non-linearity to the neural network model focuses either on enriching pooling layers [20, 21], creating new layers such as dropout layers [22] and batch normalization layers [23], or designing new activation functions [24, 25]. However, Livni et al. [26] have considered changing the way a neuron behaves by introducing a quadratic function to compute its output. By stacking layers and creating a deep network, this quadratic function enables the network to learn any polynomial of a degree not exceeding the number of layers. Moreover, they provide an algorithm that can construct the network progressively. While achieving relatively good results on various problems with a small topology and with minimal human intervention, they only dealt with the perceptron model which can be inappropriate for the problems they tackled which are computer vision problems. In fact, the perceptron model does not take into account the spatial proximity of the pixels and only considers an image as a vector with no specific spatial arrangement or relationship between neighboring pixels, which is why a convolutional model is more appropriate for these kind of problems.

Wang et al. [27], on the contrary, considered the 2D convolutional model and changed the way a neuron operates by applying a kernel function on its input which they call *kervolution*, thus, not changing the number of parameters a network needs to train, but adding a level of non-linearity that can lead to better results than regular CNNs. They used a sigmoidal, a gaussian and a polynomial kernel and studied their

influence on the accuracy measured on various datasets. Furthermore, they used well-known architectures such as ResNet [28] and modified some layers to incorporate the kervolution operator. However, they show that this operator can make the model become unstable when they introduce more complexity than what the problem requires. Although they have achieved better accuracy than state-of-the-art models, they still need to manually choose the kernel for each layer which can be inefficient due to the sheer number of possibilities they can choose from and because it can be really difficult to estimate how much non-linearity a problem needs.

Mairal [29] on the other hand, proposed a way to learn layer-wise kernels in a 2D convolutional neural network by learning a linear subspace in a Reproducing Kernel Hilbert Space [30] at each layer from which feature maps are built using kernel compositions. Although the method introduces new parameters that need to be learned during the backpropagation, its main advantage is that it gets rid of the main problem of using kernels with machine learning namely, learning and data representation decoupling. The problems that the author tackled are image classification and image super-resolution [31], and the results that were obtained outperform approaches solely based on classical convolutional neural networks. Nevertheless, due to technical limitations, the kernel learning could not be tested on large networks and its main drawback is that a pre-parametrized kernel function should be defined for each layer of the network.

However, Tran et al. [32] went even further by proposing a relaxation of the fundamental operations used in the multilayer perceptron model called Generalized Operational Perceptron (GOP) which allows changes to the summation in the linear combination between weights and inputs by any other operation such as median, maximum or product, and they call it a pool operator. Moreover, they propose the concept of nodal operators which basically applies a non-linear function on the product between the weights and the inputs. They show that this configuration surpasses the regular multilayer perceptron model on well-known classification problems, with the same number of parameters, but with a slight increase in the computational complexity. However, as a pool operator, a nodal operator and an activation function have to be chosen for every neuron in every layer, they have devised an algorithm to construct a network with the operators that should supposedly minimize the loss chosen for any given problem. Nevertheless, the main limitation of the model is that such operators need to be created and specified manually as an initial step, and that choosing an operator for every neuron is a time-consuming and compulsory preliminary step that has to be performed in order to be able to use the model and to train it.

Kiranyaz et al. [33] extended the notion of GOP to 2-dimensional signals such as images and created the Operational Neural Network (ONN) model which generalizes the 2D convolutions to any non-linear operation without adding any new parameter. They prove that ONN models can solve complex problems like image transformation, image denoising and image synthesis with a minimal topology where CNN models fail to do so with the same topology and number of parameters. They also propose an algorithm that can create homogeneous layers (all neurons inside the layer have the same pool operator, nodal operator and activation function) and choose the operators that minimize any given loss, in a greedy fashion. However, the aforementioned limitation still applies to the model since it is based on GOPs and the operator choosing algorithm does not take into account the intra-layer dependency of the so-called operators. Therefore, they proposed the concept of generative neurons in [34] to approximate nodal operators by adding learnable parameters into the network. While achieving comparable results to the ONN model, they did not get rid of the need to manually choose the pool operator and the activation function.

Nevertheless, in works [26], [27], and [29], there is still a need to manually predetermine which kernel to use on each layer, and in works [32] and [33, 34], there is a need to predetermine, for each neuron, the nodal operator, the pool operator and the activation function to use in order to create the network. The main gain of the proposed 1DPNN model is that there is no longer the need to search for a kernel that produces good results, as the model itself approximates a problem-specific polynomial kernel for each neuron.

3. Theoretical Framework

In this section, the 1DPNN will be formally defined with its relevant hyperparameters, its trainable parameters and the way to train the model with the gradient descent algorithm [2]. A theoretical analysis

of the computational complexity of the model is also made with respect to the complexity of the regular convolutional model.

3.1. 1DPNN Model Definition

The aim is to create a network whose neurons can perform non-linear filtering using a Taylor series decomposition around 0. For 1-Dimensional signals, a regular neuron in 1DCNN performs a convolution between its weight vector and its input vector whereas the neuron that needs to be modeled for 1DPNN should perform convolutions not only with its input vector but also with its exponentiation. In the following, we designate by L the number of layers of a 1DPNN. $\forall l \in \llbracket 1, L \rrbracket$, N_l is the number of neurons in layer l , D_l is the degree of the Taylor decomposition of the neurons in layer l and $\forall i \in \llbracket 1, N_l \rrbracket$, $y_i^{(l)}$ is the output vector of neuron i in layer l considered as having 1 line and M_l columns representing the output samples indexed in $\llbracket 0, M_l - 1 \rrbracket$. We consider the input layer as layer $l = 0$ with N_0 inputs in general (for a single input network, $N_0 = 1$). $\forall l \in \llbracket 0, L \rrbracket$, we construct the N_l by M_l matrix Y_l such that:

$$Y_l = \begin{bmatrix} y_1^{(l)} \\ \vdots \\ y_{N_l}^{(l)} \end{bmatrix}.$$

$\forall l \in \llbracket 1, L \rrbracket$, $\forall (i, j, d) \in \llbracket 1, N_l \rrbracket \times \llbracket 1, N_{l-1} \rrbracket \times \llbracket 1, D_l \rrbracket$, $w_{ijd}^{(l)}$ is the weight vector of neuron i in layer l corresponding to the exponent d and to the output of neuron j in layer $l - 1$ considered as having 1 line and K_l columns indexed in $\llbracket 0, K_l - 1 \rrbracket$. $\forall l \in \llbracket 1, L \rrbracket$, $\forall (i, d) \in \llbracket 1, N_l \rrbracket \times \llbracket 1, D_l \rrbracket$, we construct the N_{l-1} by K_l matrix $W_{id}^{(l)}$ such that:

$$W_{id}^{(l)} = \begin{bmatrix} w_{i1d}^{(l)} \\ \vdots \\ w_{iN_{l-1}d}^{(l)} \end{bmatrix}.$$

$\forall l \in \llbracket 1, L \rrbracket$, $\forall i \in \llbracket 1, N_l \rrbracket$, $b_i^{(l)}$ is the bias of neuron i in layer l and $f_i^{(l)}$ is a differentiable function called the activation function of neuron i in layer l such that $y_i^{(l)} = f_i^{(l)}(x_i^{(l)})$ where $x_i^{(l)}$ is the pre-activation output of neuron i in layer l .

Definition 1. The output of a neuron in the 1DPNN is defined as such:

$$\forall l \in \llbracket 1, L \rrbracket, \forall i \in \llbracket 1, N_l \rrbracket, y_i^{(l)} = f_i^{(l)} \left(\sum_{d=1}^{D_l} W_{id}^{(l)} * Y_{l-1}^d + b_i^{(l)} \right) = f_i^{(l)}(x_i^{(l)}), \quad (1)$$

where $*$ is the convolution operator, $Y_{l-1}^d = \underbrace{Y_{l-1} \odot \cdots \odot Y_{l-1}}_{d \text{ times}}$, and \odot is the Hadamard product.

Remark 1. As stated above, the whole focus of this work is to learn the best polynomial function in each neuron for a given problem, which is entirely defined by the weights $W_{id}^{(l)}$ associated with Y_{l-1} to the power of d .

Remark 2. Since the 1DPNN neuron creates a polynomial function using the weights $W_{id}^{(l)}$, the activation function $f_i^{(l)}$ can seem unnecessary to define, and can be replaced by the identity function. However, in the context of the 1DPNN model, the activation function plays the role of a bounding function, meaning that it can be used to control the range of the values of the created polynomial function.

3.2. 1DPNN Model Training

In order to enable the weights of the model to be updated so that it learns, we need to define a loss function that measures whether the output of the network is close or far from the output that is desired since it is a supervised model. We denote by Y the desired output, by \hat{Y} the output that is produced by the network, and by $\epsilon(Y, \hat{Y})$ the loss between the desired output and the estimated output. ϵ needs to be differentiable since the estimation of its derivative with respect to different variables is the key of learning the weights due to the fact that gradient descent is used as a numeric optimization technique.

3.2.1. Gradient Descent Algorithm

Given a function $\phi : \mathbb{R}^N \times \mathbb{R}^P \rightarrow \mathbb{R}^M$, where $(M, N, P) \in \mathbb{N}^{*3}$, the input is a tuple $X = (X_1, \dots, X_N) \in \mathbb{R}^N$, and the parameters are $\theta = (\theta_1, \dots, \theta_P)$; we consider a desired output from X given ϕ called Y where $Y \in \mathbb{R}^M$. The objective is to estimate θ so that $\epsilon(Y, \phi(X, \theta))$ is minimum where $\epsilon : \mathbb{R}^M \times \mathbb{R}^M \rightarrow \mathbb{R}_+$ is a differentiable loss function. Gradient descent [35] is an algorithm that iteratively estimates new values of θ for T iterations or until a target loss ϵ_t is attained. $\forall t \in \llbracket 0, T \rrbracket$, $\hat{\theta}^{(t)} = (\hat{\theta}_1^{(t)}, \dots, \hat{\theta}_P^{(t)})$ is the estimated value of θ at iteration t . Given an initial value $\hat{\theta}^{(0)}$, and a learning rate $\eta \in (0, 1]$, the gradient descent estimations are

$$\forall t \in \llbracket 0, T - 1 \rrbracket, \hat{\theta}^{(t+1)} = \hat{\theta}^{(t)} - \eta \nabla_{\theta} \epsilon(\hat{\theta}^{(t)}),$$

where $\nabla_{\theta} \epsilon(\hat{\theta}^{(t)})$ is the gradient of ϵ with respect to θ applied on $\hat{\theta}^{(t)}$. In the case of the 1DPNN, the parameters are the weights and the biases so there is a need to estimate the weight gradients $\frac{\partial \epsilon}{\partial w_{ijd}^{(l)}}$ and the bias derivatives $\frac{\partial \epsilon}{\partial b_i^{(l)}}$, $\forall l \in \llbracket 1, L \rrbracket, \forall (i, j, d) \in \llbracket 1, N_l \rrbracket \times \llbracket 1, N_{l-1} \rrbracket \times \llbracket 1, D_l \rrbracket$.

3.2.2. Weight Gradient Estimation

In order for the weights to be updated using the Gradient Descent algorithm, there is a need to estimate the contribution of each weight of each neuron in the loss by means of calculating the gradient.

Proposition 1. The gradient of the loss with respect to the weights of a 1DPNN neuron can be estimated using the following formula:

$$\forall l \in \llbracket 1, L \rrbracket, \forall (i, j, d) \in \llbracket 1, N_l \rrbracket \times \llbracket 1, N_{l-1} \rrbracket \times \llbracket 1, D_l \rrbracket,$$

$$\frac{\partial \epsilon}{\partial w_{ijd}^{(l)}} = \left(\frac{\partial \epsilon}{\partial y_i^{(l)}} \odot \frac{\partial y_i^{(l)}}{\partial x_i^{(l)}} \right) * \left(y_j^{(l-1)} \right)^d = \frac{\partial \epsilon}{\partial x_i^{(l)}} * \left(y_j^{(l-1)} \right)^d, \quad (2)$$

where:

- $\frac{\partial y_i^{(l)}}{\partial x_i^{(l)}} = \frac{\partial f_i^{(l)}}{\partial x_i^{(l)}}(x_i^{(l)})$ is the derivative of the activation function of neuron i in layer l with respect to $x_i^{(l)}$.
- $\frac{\partial \epsilon}{\partial y_i^{(l)}}$ is the gradient of the loss with respect to the output of neuron i in layer l , that we call the output gradient.

Proof of Proposition 1. To estimate the weight gradients, we use the chain-rule such that:

$$\forall l \in \llbracket 1, L \rrbracket, \forall (i, j, k, d) \in \llbracket 1, N_l \rrbracket \times \llbracket 1, N_{l-1} \rrbracket \times \llbracket 0, K_l - 1 \rrbracket \times \llbracket 1, D_l \rrbracket,$$

$$\frac{\partial \epsilon}{\partial w_{ijd}^{(l)}}(k) = \sum_{m=0}^{M_l-1} \left(\frac{\partial \epsilon}{\partial y_i^{(l)}} \odot \frac{\partial y_i^{(l)}}{\partial x_i^{(l)}} \right)(m) \cdot \frac{\partial x_i^{(l)}}{\partial w_{ijd}^{(l)}}(m). \quad (3)$$

From Eq. (1), we can write:

$$\forall l \in \llbracket 1, L \rrbracket, \forall (i, m, d) \in \llbracket 1, N_l \rrbracket \times \llbracket 0, M_l - 1 \rrbracket \times \llbracket 1, D_l \rrbracket,$$

$$x_i^{(l)}(m) = \sum_{j'=1}^{N_{l-1}} \sum_{d'=1}^{D_l} \sum_{k'=0}^{K_l-1} w_{ij'd'}^{(l)}(k') \left(y_{j'}^{(l-1)} \right)^{d'} (m + k'),$$

from which we deduce:

$$\forall l \in \llbracket 1, L \rrbracket, \forall (i, j, m, k, d) \in \llbracket 1, N_l \rrbracket \times \llbracket 1, N_{l-1} \rrbracket \times \llbracket 0, M_l - 1 \rrbracket \times \llbracket 0, K_l - 1 \rrbracket \times \llbracket 1, D_l \rrbracket,$$

$$\frac{\partial x_i^{(l)}}{\partial w_{ijd}^{(l)}}(m) = \left(y_j^{(l-1)} \right)^d (m + k). \quad (4)$$

When injecting Eq. (4) in Eq. (3), we find that:

$$\forall l \in \llbracket 1, L \rrbracket, \forall (i, j, k, d) \in \llbracket 1, N_l \rrbracket \times \llbracket 1, N_{l-1} \rrbracket \times \llbracket 0, K_l - 1 \rrbracket \times \llbracket 1, D_l \rrbracket,$$

$$\frac{\partial \epsilon}{\partial w_{ijd}^{(l)}}(k) = \sum_{m=0}^{M_l-1} \left(\frac{\partial \epsilon}{\partial y_i^{(l)}} \odot \frac{\partial y_i^{(l)}}{\partial x_i^{(l)}} \right)(m) \cdot \left(y_j^{(l-1)} \right)^d (m + k),$$

which is equivalent to:

$$\forall l \in \llbracket 1, L \rrbracket, \forall (i, j, d) \in \llbracket 1, N_l \rrbracket \times \llbracket 1, N_{l-1} \rrbracket \times \llbracket 1, D_l \rrbracket,$$

$$\frac{\partial \epsilon}{\partial w_{ijd}^{(l)}} = \left(\frac{\partial \epsilon}{\partial y_i^{(l)}} \odot \frac{\partial y_i^{(l)}}{\partial x_i^{(l)}} \right) * \left(y_j^{(l-1)} \right)^d = \frac{\partial \epsilon}{\partial x_i^{(l)}} * \left(y_j^{(l-1)} \right)^d. \quad (5)$$

Remark 3. The weight gradient estimation of a 1DPNN neuron is equivalent to that of a 1DCNN neuron when $D_l = 1$. This was to be expected as the former is only a mere extension of the latter.

Remark 4. The output gradient can easily be determined for the last layer since $\hat{Y} = Y_L$ which makes the loss directly dependent on Y_L . However, it can not be determined as easily for the other layers since the loss is indirectly dependent on their outputs.

3.2.3. Output Gradient Estimation

As stated in Remark 4, there is a need to find a way to estimate the gradient of the loss with respect to the inner layers' outputs in order to estimate the weight gradients of their neurons as in Eq. (2).

Proposition 2. The output gradient of a neuron in an inner layer can be estimated using the following formula:

$$\forall l \in \llbracket 1, L - 1 \rrbracket, j \in \llbracket 1, N_l \rrbracket,$$

$$\frac{\partial \epsilon}{\partial y_j^{(l)}} = \sum_{d=1}^{D_l} d \left(\sum_{i=1}^{N_{l+1}} \tilde{w}_{ijd}^{(l+1)} * \frac{\overset{\circ}{\partial} \epsilon}{\partial x_i^{(l+1)}} \right) \odot \left(y_j^{(l)} \right)^{d-1}, \quad (6)$$

where:

- $\forall k \in \llbracket 0, K_{l+1} - 1 \rrbracket, \tilde{w}_{ijd}^{(l+1)}(k) = w_{ijd}^{(l+1)}(K_{l+1} - 1 - k).$
- $\forall m \in \llbracket 0, M_l - 1 \rrbracket, \frac{\partial \epsilon}{\partial x_i^{(l+1)}}(m) = \begin{cases} \frac{\partial \epsilon}{\partial x_i^{(l+1)}}(m - K_{l+1}) & \text{if } m \in \llbracket K_{l+1}, M_{l+1} + K_{l+1} - 1 \rrbracket \\ 0 & \text{else} \end{cases}.$

Proof of Proposition 2. Since Y_{l+1} is directly computed from $Y_l, \forall l \in \llbracket 1, L - 1 \rrbracket$, we can assume that ultimately, the last layer's output Y_L is totally dependent on Y_{l+1} so that we can write:

$$\forall l \in \llbracket 1, L - 1 \rrbracket, \epsilon(Y, \hat{Y}) = \epsilon(Y, \psi_{l+1}(Y_{l+1})), \quad (7)$$

where Y is a given desired output and ψ_{l+1} is the application of Eq. (1) from layer $l + 1$ to layer L . From Eq. (7) we can write the differential of ϵ as such:

$$\forall l \in \llbracket 1, L - 1 \rrbracket, d\epsilon = \sum_{i=1}^{N_{l+1}} \frac{\partial \epsilon}{\partial y_i^{(l+1)}} \odot dy_i^{(l+1)}. \quad (8)$$

We can then derive the general expression of the output gradient of any neuron in layer l as such:

$$\forall l \in \llbracket 1, L - 1 \rrbracket, j \in \llbracket 1, N_l \rrbracket, \frac{\partial \epsilon}{\partial y_j^{(l)}} = \sum_{i=1}^{N_{l+1}} \frac{\partial \epsilon}{\partial y_i^{(l+1)}} \odot \frac{\partial y_i^{(l+1)}}{\partial y_j^{(l)}} = \sum_{i=1}^{N_{l+1}} \frac{\partial \epsilon}{\partial y_i^{(l+1)}} \odot \frac{\partial y_i^{(l+1)}}{\partial x_i^{(l+1)}} \odot \frac{\partial x_i^{(l+1)}}{\partial y_j^{(l)}}.$$

This expression can be qualitatively interpreted as finding the contribution of each sample in $y_j^{(l)}$ in the loss by finding its contribution to every output vector in layer $l + 1$. Considering a layer $l \in \llbracket 1, L - 1 \rrbracket$, a neuron j in layer l , and a neuron i in layer $l + 1$, a sample $m \in \llbracket 0, M_l - 1 \rrbracket$ in $y_j^{(l)}$ contributes to $x_i^{(l+1)}$ in the following samples:

$$\forall l \in \llbracket 1, L - 1 \rrbracket, \forall (i, m, k, d) \in \llbracket 1, N_{l+1} \rrbracket \times \llbracket 0, M_l - 1 \rrbracket \times \llbracket k_{lm}, k'_{lm} \rrbracket \times \llbracket 1, D_{l+1} \rrbracket, \\ x_i^{(l+1)}(m - k) = \sum_{j'=1}^{N_l} \sum_{d=1}^{D_{l+1}} \sum_{k'=0}^{K_{l+1}-1} w_{ij'd}^{(l+1)}(k') \left(y_{j'}^{(l)}\right)^d (m - k + k'),$$

where $\forall l \in \llbracket 1, L - 1 \rrbracket, k_{lm} = \max(0, m - M_{l+1} + 1)$ and $k'_{lm} = \min(m, K_{l+1} - 1)$. We can then determine the exact contributions of $y_j^{(l)}(m)$ in $x_i^{(l+1)}$ as such:

$$\forall l \in \llbracket 1, L - 1 \rrbracket, \forall (i, j, m, k, d) \in \llbracket 1, N_{l+1} \rrbracket \times \llbracket 1, N_l \rrbracket \times \llbracket 0, M_l - 1 \rrbracket \times \llbracket k_{lm}, k'_{lm} \rrbracket \times \llbracket 1, D_{l+1} \rrbracket, \\ \frac{\partial x_i^{(l+1)}}{\partial y_j^{(l)}}(m - k) = \sum_{d=1}^{D_{l+1}} d \cdot w_{ij'd}^{(l+1)}(k) \left(y_j^{(l)}\right)^{d-1}(m). \quad (9)$$

Therefore, we can finally determine the full expression of the output gradient for each sample:

$$\forall l \in \llbracket 1, L - 1 \rrbracket, (j, m) \in \llbracket 1, N_l \rrbracket \times \llbracket 0, M_l - 1 \rrbracket, \\ \frac{\partial \epsilon}{\partial y_j^{(l)}}(m) = \sum_{i=1}^{N_{l+1}} \sum_{k=k_{lm}}^{k'_{lm}} \sum_{d=1}^{D_l} d \cdot \left(\frac{\partial \epsilon}{\partial y_i^{(l+1)}} \odot \frac{\partial y_i^{(l+1)}}{\partial x_i^{(l+1)}} \right) (m - k) w_{ij'd}^{(l+1)}(k) \left(y_j^{(l)}\right)^{d-1}(m). \quad (10)$$

Eq. (10) can be decomposed as the sum along i and d of the product of $\left(y_j^{(l)}\right)^{d-1}$ with the correlation between $\frac{\partial \epsilon}{\partial x_i^{(l+1)}}$ and $w_{ij'd}^{(l+1)}$, the correlation being a rotated version of the convolution where the samples

of the weights are considered in an inverted order to that of the convolution. Therefore, a correlation can be transformed into a convolution by considering the rotated weights $\tilde{w}_{ijd}^{(l+1)}$ defined as such:

$$\forall k \in \llbracket 0, K_{l+1} - 1 \rrbracket, \tilde{w}_{ijd}^{(l+1)}(k) = w_{ijd}^{(l+1)}(K_{l+1} - 1 - k).$$

However, we can only perform a valid convolution when $k_{lm} = 0$ and $k'_{lm} = K_{l+1} - 1$. Thus, to obtain a valid convolution otherwise, we consider the zero-padded version of $\frac{\partial \epsilon}{\partial x_i^{(l+1)}}$ designated by $\frac{\overset{\circ}{\partial} \epsilon}{\partial x_i^{(l+1)}}$ and defined as such:

$$\forall m \in \llbracket 0, M_l - 1 \rrbracket, \frac{\overset{\circ}{\partial} \epsilon}{\partial x_i^{(l+1)}}(m) = \begin{cases} \frac{\partial \epsilon}{\partial x_i^{(l+1)}}(m - K_{l+1}) & \text{if } m \in \llbracket K_{l+1}, M_{l+1} + K_{l+1} - 1 \rrbracket \\ 0 & \text{else} \end{cases}.$$

Finally, we can obtain the desired expression by considering the rotated version of the weights, and the zero-padded version of the gradient of the error with respect to $x_i^{(l+1)}$ in Eq. (10).

Remark 5. The main difference between the output gradient estimation of a 1DPNN inner layer's neuron and that of a 1DCNN inner layer's neuron is that in the former, the gradient depends on the output values of the considered layer and in the latter, it does not. By injecting Eq. (6) in Eq. (2), we notice that, unlike a 1DCNN neuron, the weight gradient of a 1DPNN inner layer's neuron carry the information of its output values as well as its previous layer's output values.

3.2.4. Bias Gradient Estimation

The bias is a parameter whose contribution to the loss needs to be estimated in order to properly train the model.

Proposition 3. The bias gradient of a 1DPNN neuron can be estimated using the following formula:

$$\forall l \in \llbracket 1, L \rrbracket, \forall i \in \llbracket 1, N_l \rrbracket, \frac{\partial \epsilon}{\partial b_i^{(l)}} = \sum_{m=0}^{M_l-1} \left(\frac{\partial \epsilon}{\partial y_i^{(l)}} \odot \frac{\partial y_i^{(l)}}{\partial x_i^{(l)}} \right) (m) = \sum_{m=0}^{M_l-1} \frac{\partial \epsilon}{\partial x_i^{(l)}}(m).$$

Proof of Proposition 3. Using the differential of ϵ , we can determine the gradient of the loss with respect to the bias as such:

$$\forall l \in \llbracket 1, L \rrbracket, \forall i \in \llbracket 1, N_l \rrbracket, \frac{\partial \epsilon}{\partial b_i^{(l)}} = \sum_{m=0}^{M_l-1} \left(\frac{\partial \epsilon}{\partial y_i^{(l)}} \odot \frac{\partial y_i^{(l)}}{\partial x_i^{(l)}} \odot \frac{\partial x_i^{(l)}}{\partial b_i^{(l)}} \right) (m).$$

And since from Eq. (1), we can notice that $\frac{\partial x_i^{(l)}}{\partial b_i^{(l)}}(m) = 1, \forall l \in \llbracket 1, L \rrbracket, \forall (i, m) \in \llbracket 1, N_l \rrbracket \times \llbracket 0, M_l - 1 \rrbracket$, we obtain the desired expression.

Remark 6. The bias gradient formula of a 1DPNN neuron is the same as that of a 1DCNN neuron regardless of the degree of the polynomial approximation.

3.2.5. Training Procedure

Given a tuple (X, Y) representing an input and a desired output, we generate \hat{Y} using a defined architecture of the 1DPNN, then calculate $\frac{\partial \epsilon}{\partial Y_L}$ directly from the loss expression, in order to determine the

weight gradients and the bias gradients for the output layer. Then using $\frac{\partial \epsilon}{\partial Y_L}$ and Eq. (6), calculate the output gradients, the weight gradients and the bias gradients of the previous layer. Repeat the process until reaching the first layer. After computing the gradients, we use gradient descent to update the weights as such:

$$\forall l \in \llbracket 1, L \rrbracket, \forall (i, j, d) \in \llbracket 1, N_l \rrbracket \times \llbracket 1, N_{l-1} \rrbracket \times \llbracket 1, D_l \rrbracket, \left(w_{ijd}^{(l)}\right)^{(t+1)} = \left(w_{ijd}^{(l)}\right)^{(t)} - \eta \frac{\partial \epsilon}{\partial w_{ijd}^{(l)}}, \quad (11)$$

where η is the learning rate and t is the epoch. The same goes for the updating the biases:

$$\forall l \in \llbracket 1, L \rrbracket, \forall i \in \llbracket 1, N_l \rrbracket, \left(b_i^{(l)}\right)^{(t+1)} = \left(b_i^{(l)}\right)^{(t)} - \eta \frac{\partial \epsilon}{\partial b_i^{(l)}}.$$

3.3. 1DPNN Weight Initialization

Since the 1DPNN model uses polynomials to generate non-linear filtering, it is highly likely that, due to the fact that every feature map of every layer is raised to a power higher than 1, the weight updates become exponentially big (gradient explosion) or exponentially small (gradient vanishing), depending on the nature of the activation functions that are used. To remedy that, the weights have to be initialized in a way that the highest power of any feature map is associated with the lowest weight values.

Definition 2. Let $\mathcal{R}(\alpha_l), l \in \llbracket 1, L \rrbracket$ be a probability law with a parameter vector α_l used to initialize the weights of any layer l . The proposed weight initialization is defined as such:

$$\forall l \in \llbracket 1, L \rrbracket, (i, j, d) \in \llbracket 1, N_l \rrbracket \times \llbracket 1, N_{l-1} \rrbracket \times \llbracket 1, D_l \rrbracket, w_{ijd}^{(l)} \sim \frac{\mathcal{R}(\alpha_l)}{d!}.$$

Remark 7. This initialization offers the advantage of allowing the use of any known deep-learning initialization scheme such as the Glorot Normalized Uniform Initialization [36] while adapting it to the weights associated with any degree. However, this does not ensure that there will be no gradient explosion as it only provides an initial insight on how the weights should evolve. Completely avoiding gradient explosion can be achieved by either choosing activation functions bounded between -1 and 1, by performing weight or gradient clipping or by using weight or activity regularization.

3.4. 1DPNN Theoretical Computational Complexity Analysis

The use of polynomial approximations in the 1DPNN model introduces a level of complexity that has to be quantified in order to estimate the gain of using it against using the regular convolutional model. Therefore, a thorough analysis is conducted with the aim to determine the complexity of the 1DPNN model with respect to the complexity of the 1DCNN model for both the forward propagation and the learning process (forward propagation + backpropagation).

Definition 3. Let γ be a mathematical expression that can be brought to a combination of summations and products. We define \mathcal{C} as a function that takes as input a mathematical expression such as γ and outputs an integer designating the number of operations performed to calculate that expression so that $\mathcal{C}(\gamma) \in \mathbb{N}$.

Example 1. Let $N \in \mathbb{N}^*$ and $\gamma = \sum_{i=1}^N i^3$, then $\mathcal{C}(\gamma) = 2N + N - 1 = 3N - 1$ because $N - 1$ summations are performed, and 2 products are performed N times.

Example 2. $\forall z \in \mathbb{C}, 0 \leq \mathcal{C}(z) \leq 2$ because a complex number can be written as $z = a + ib, (a, b) \in \mathbb{R}^2$.

Remark 8. \mathcal{C} does not take into account any possible optimization such as the one for the exponentiation in Example 1 which can have a complexity of $\mathcal{O}(\log_2 m)$ where m is the exponent, nor does it take into account any possible simplification of a mathematical expression such as $\sum_{i=1}^N i^3 = \frac{N^2(N+1)^2}{4}$. Therefore, \mathcal{C} provides an upper bound complexity that is independent of any implementation.

Since the smallest computational unit in both models is the neuron, the complexity is calculated at its level for every operation performed during the forward propagation and the backpropagation. Moreover, every 1DPNN operation's complexity denoted by \mathcal{C}_p is calculated as a function of the corresponding 1DCNN operation's complexity denoted by \mathcal{C}_c since the aim is to compare both models with each others.

3.4.1. Forward Propagation Complexity

The forward propagation complexity is a measure relevant to the estimation of how complex a trained 1DPNN neuron is and can provide an insight on how complex it is to use a trained model compared to using a trained 1DCNN model.

Proposition 4. The computational complexity a 1DPNN neuron's forward propagation with respect to that of a 1DCNN neuron is given by the following formula:

$$\forall l \in \llbracket 1, L \rrbracket, \forall i \in \llbracket 1, N_l \rrbracket, \mathcal{C}_p \left(y_i^{(l)} \right) = D_l \mathcal{C}_c \left(y_i^{(l)} \right) + (D_l - 1) \left(\frac{1}{2} M_{l-1} N_{l-1} D_l - 2M_l \right). \quad (12)$$

Proof of Proposition 4. The 1DPNN forward propagation is fully defined by Eq. (1) which can also be interpreted as the 1DCNN forward propagation if the degree of the polynomials is 1. Therefore, we can determine the 1DPNN complexity as a function of the 1DCNN complexity by first determining the complexity of $x_i^{(l)}$ before adding the biases as such:

$$\begin{aligned} \forall l \in \llbracket 1, L \rrbracket, \forall i \in \llbracket 1, N_l \rrbracket, \\ \mathcal{C}_p \left(x_i^{(l)} - b_i^{(l)} \right) = \sum_{d=1}^{D_l} \left(\mathcal{C}_c \left(x_i^{(l)} - b_i^{(l)} \right) + (d-1) M_{l-1} N_{l-1} \right) = D_l \mathcal{C}_c \left(x_i^{(l)} - b_i^{(l)} \right) + \frac{1}{2} D_l (D_l - 1) M_{l-1} N_{l-1}. \end{aligned} \quad (13)$$

Assuming that the activation functions are atomic meaning that their complexity is $\mathcal{O}(1)$, we have:

$$\forall l \in \llbracket 1, L \rrbracket, \forall i \in \llbracket 1, N_l \rrbracket, \begin{cases} \mathcal{C}_c \left(x_i^{(l)} \right) &= \mathcal{C}_c \left(x_i^{(l)} - b_i^{(l)} \right) + M_l \\ \mathcal{C}_c \left(y_i^{(l)} \right) &= \mathcal{C}_c \left(x_i^{(l)} \right) + M_l \end{cases} \text{ and } \begin{cases} \mathcal{C}_p \left(x_i^{(l)} \right) &= \mathcal{C}_p \left(x_i^{(l)} - b_i^{(l)} \right) + M_l \\ \mathcal{C}_p \left(y_i^{(l)} \right) &= \mathcal{C}_p \left(x_i^{(l)} \right) + M_l \end{cases}. \quad (14)$$

By using the relationships in Eq. (14) in Eq. (13), we obtain the desired expression.

Remark 9. Eq. (12) shows that the forward propagation's complexity of the 1DPNN does not scale linearly with the degrees of the polynomials, which means that a 1DPNN neuron with degree D_l is more computationally complex than D_l 1DCNN neurons despite having less trainable parameters (same number of weights but only 1 bias). However, this complexity can become linear since Y_{l-1}^d can be calculated only once, stored in memory and used for all neurons in layer l .

3.4.2. Learning Complexity

The learning complexity is a measure relevant to the estimation of how complex it is to train a 1DPNN neuron and can provide an overall insight on how complex a model is to train compared to training a 1DCNN model. Since the learning process of the inner layers' neurons is more complex than the output layer's neurons which can learn faster by estimating the output gradient directly from the loss function, the learning complexity will only be determined for the inner layers' neurons.

Proposition 5. The computational complexity of the learning process of a 1DPNN inner layer's neuron denoted by $\mathcal{L}_p^{(l)}$ is given by the following formula:

$$\forall l \in \llbracket 1, L-1 \rrbracket, \mathcal{L}_p^{(l)} = D_l \mathcal{L}_c^{(l)} + (D_l - 1) \left(\left(M_{l-1} N_{l-1} + \frac{1}{2} M_l \right) D_l - M_l \right), \quad (15)$$

where $\mathcal{L}_c^{(l)}$ is the learning complexity of a 1DCNN neuron in a layer l .

Proof of Proposition 5. The difference between the two models in the backpropagation phase resides in the weight gradient estimation and the output gradient estimation. In fact, the bias gradient estimation is the same for both models so there is no need to quantify its complexity. Since the weight gradient estimation is dependent on the output gradient estimation, the output gradient estimation will be quantified first. From Eq.(6), we can quantify the output gradient estimation complexity for the 1DPNN model as such:

$$\forall l \in \llbracket 1, L-1 \rrbracket, j \in \llbracket 1, N_l \rrbracket, \\ \mathcal{C}_p \left(\frac{\partial \epsilon}{\partial y_j^{(l)}} \right) = \mathcal{C}_c \left(\frac{\partial \epsilon}{\partial y_j^{(l)}} \right) + \sum_{d=2}^{D_l} \left(\mathcal{C}_c \left(\frac{\partial \epsilon}{\partial y_j^{(l)}} \right) + 2M_l + (d-2)M_l \right) = D_l \mathcal{C}_c \left(\frac{\partial \epsilon}{\partial y_j^{(l)}} \right) + \frac{1}{2}(D_l + 2)(D_l - 1)M_l.$$

Since the 1DPNN neuron introduces D_l times more weights than the 1DCNN neuron, the complexity of calculating the weight gradients for a pair of neurons (i, j) as in Eq. (2) is the sum of their corresponding weight gradients with respect to the degree, as such:

$$\forall l \in \llbracket 1, L \rrbracket, \forall (i, j) \in \llbracket 1, N_l \rrbracket \times \llbracket 1, N_{l-1} \rrbracket, \\ \mathcal{C}_p \left(\frac{\partial \epsilon}{\partial w_{ij}^{(l)}} \right) = \sum_{d=1}^{D_l} \mathcal{C}_p \left(\frac{\partial \epsilon}{\partial w_{ij}^{(l)}} \right) = \sum_{d=1}^{D_l} \left(\mathcal{C}_c \left(\frac{\partial \epsilon}{\partial w_{ij}^{(l)}} \right) + (d-1)M_{l-1} \right) = D_l \mathcal{C}_c \left(\frac{\partial \epsilon}{\partial w_{ij}^{(l)}} \right) + \frac{1}{2}D_l(D_l - 1)M_{l-1}.$$

Since one 1DPNN neuron in a layer l has D_l times more weights than a 1DCNN neuron, its weight update complexity is D_l times that of the 1DCNN. Therefore, the complexity of Eq. (11) is:

$$\forall l \in \llbracket 1, L \rrbracket, \forall (i, j) \in \llbracket 1, N_l \rrbracket \times \llbracket 1, N_{l-1} \rrbracket, \mathcal{C}_p \left(\left(w_{ij}^{(l)} \right)^{(t+1)} \right) = D_l \mathcal{C}_c \left(\left(w_{ij}^{(l)} \right)^{(t+1)} \right).$$

From the above expressions, we can determine the learning complexity of any neuron which will be the sum of the forward propagation complexity and the backward propagation complexity. Therefore, the learning complexity denoted by $\mathcal{L}_{p,i}^{(l)}$ of a 1DPNN inner layer's neuron is:

$$\forall l \in \llbracket 1, L-1 \rrbracket, i \in \llbracket 1, N_l \rrbracket, \mathcal{L}_{p,i}^{(l)} = \mathcal{C}_p \left(y_i^{(l)} \right) + \mathcal{C}_p \left(\frac{\partial \epsilon}{\partial y_i^{(l)}} \right) + \sum_{j=1}^{N_{l-1}} \left(\mathcal{C}_p \left(\frac{\partial \epsilon}{\partial w_{ij}^{(l)}} \right) + \mathcal{C}_p \left(\left(w_{ij}^{(l)} \right)^{(t+1)} \right) \right).$$

Since we suppose that the network is fully connected, $\mathcal{L}_{p,i}^{(l)}$ does not depend on i , thus we can replace it by $\mathcal{L}_p^{(l)}$. Therefore, by replacing each complexity in the above equation by their full expressions, we obtain the desired expression where:

$$\forall l \in \llbracket 1, L-1 \rrbracket, i \in \llbracket 1, N_l \rrbracket, \mathcal{L}_c^{(l)} = \mathcal{C}_c \left(y_i^{(l)} \right) + \mathcal{C}_c \left(\frac{\partial \epsilon}{\partial y_i^{(l)}} \right) + \sum_{j=1}^{N_{l-1}} \left(\mathcal{C}_c \left(\frac{\partial \epsilon}{\partial w_{ij}^{(l)}} \right) + \mathcal{C}_c \left(\left(w_{ij}^{(l)} \right)^{(t+1)} \right) \right).$$

4. Implementation

This section describes the application programming interface (API) used to implement the 1DPNN model as well as an evaluation of the implementation in the form of an experimental computational complexity analysis for the forward propagation and the learning process of a 1DPNN neuron.

4.1. Keras Tensorflow API Implementation

Tensorflow [37] is an API created by Google that is widely used for graphics processing unit (GPU)-based symbolic computation and especially for neural networks. It allows the implementation of a wide range of models and automatically takes into account the usual derivatives without the need to define them manually. However, Tensorflow is a low-level API that involves a lot of coding and memory management to define a simple model. The 1DPNN model is mainly based on convolutions between inputs and filters, so it can be considered as an extension of the basic 1DCNN with slight changes. Therefore, there is no need to use such a low-level API like Tensorflow or Cuda to define the 1DPNN, so the Keras API was used to implement the model.

Keras [38] is a high level API built on top of Tensorflow that provides an abstraction of the internal operations performed to compute gradients or anything related. Keras allows to build a network as a combination of layers whether they are stacked sequentially or not. It uses the concept of layer which is the key element to perform any operation and allows the definition of custom layers that can jointly be used with predefined layers, thus, allowing to create a heterogeneous network composed of different types of layers. In Keras, there is only the need to define the forward propagation of 1DPNN since convolutions and exponents are considered basic operations, and the API takes care of storing the gradients and using them to calculate the weight updates.

4.2. Experimental Computational Complexity Analysis

In order to evaluate the efficiency of the implementation, we compare the forward propagation complexity and the learning process complexity of a 1DPNN neuron with the respective theoretical upper bound complexities determined in Section 3.4, as well as with a 1DCNN neuron's complexity, and a 1DPNN-equivalent neuron by varying the degrees of the polynomials in a given range. This experimental analysis is made to show that the theoretical complexity is indeed an upper bound and that, as stated in Section 3.4, a 1DPNN neuron with a degree D is actually more complex than D 1DCNN neurons, which is the genesis of the idea of a 1DPNN-equivalent neuron.

4.2.1. 1DPNN-Equivalent Network

Theorem 1. Any 1DPNN with $L \geq 1$ layers can be transformed into a 1DCNN with $L + 1$ layers that has the same number of parameters as the 1DPNN.

Proof of Theorem 1. Let $L \in \mathbb{N}^*$ be the number of layers of a 1DPNN and $\forall l \in \llbracket 1, L + 1 \rrbracket$, let N'_l be the number of neurons in a 1DCNN layer. Given any inner 1DPNN layer, we can create a 1DCNN layer that has the same number of parameters using the equality between the number of parameters of each model's layer as such:

$$\forall l \in \llbracket 1, L - 1 \rrbracket, N'_l N'_{l-1} K_l + N'_l = N_l N_{l-1} K_l D_l + N_l,$$

where $N'_0 = N_0$ since the input layer remains the same. We then determine N'_l from that equation as such:

$$\forall l \in \llbracket 1, L - 1 \rrbracket, N'_l = \left\lfloor \frac{N_l(N_{l-1}K_l D_l + 1)}{N'_{l-1}K_l + 1} + \frac{1}{2} \right\rfloor, \quad (16)$$

where N'_l is rounded by adding $1/2$ and applying the floor function since it should be an integer. If we determine N'_L in the same manner as we determine the number of neurons in the inner layers, we will change the number of neurons in the output layer of the 1DCNN, which is not a desired effect. To remedy that problem, we add another 1DCNN layer with $N'_{L+1} = N_L$ neurons having a filter size of 1 in the 1DCNN, and we adjust the number of neurons in layer L so that the number of parameters in layer L and layer $L + 1$ equals the number of parameters in the 1DPNN layer L using the following equality:

$$N'_L N'_{L-1} K_L + N'_L + N_L N'_L + N_L = N_L N_{L-1} K_L D_L + N_L.$$

By extracting N'_L from this expression and by rounding it, we end up with

$$N'_L = \left\lfloor \frac{N_L N_{L-1} K_L D_L}{N'_{L-1} K_L + N_L + 1} + \frac{1}{2} \right\rfloor. \quad (17)$$

Remark 10. We call any 1DCNN recurrently constructed using the aforementioned theorem and Eqs. (16) and (17) a 1DPNN-equivalent network because it has the same number of parameters as the 1DPNN it was constructed from. However, their respective search spaces and computational complexities are generally not equivalent.

Remark 11. In a 1DPNN having only 1 layer ($L = 1$), $\left\lfloor \frac{N'_L}{N_L} + \frac{1}{2} \right\rfloor$ 1DCNN neurons are considered equivalent to only one 1DPNN neuron, and thus comes the concept of a 1DPNN-equivalent neuron. Comparing a 1DPNN neuron with its equivalent 1DCNN neuron is indeed helpful to determine the gain or loss of using one over the other by providing an insight on how to estimate the balance between searching features in a more complex search space and searching less complex features in less time.

4.2.2. Experimental Setup

Since the implementation is GPU-based, it is very difficult to estimate the actual execution time of a mathematical operation since it can be split among parallel execution kernels and since the memory bandwidth greatly impacts it. Nevertheless, for a given amount of data, we can roughly estimate how fast a mathematical operation was performed by running it multiple times and averaging. However, that estimate also includes accesses to the memory which are the slowest operations that can run on a GPU, and does not provide a real estimation on how fast an operation was performed nor does it align with the true computational power of the so-called GPU.

Despite this limitation, a rough estimate is used to determine the execution times of a 1DPNN neuron, a 1DCNN neuron and a 1DPNN-equivalent neuron with different hyperparameters. Various networks with 2 layers serving as a basis for the complexity estimation are created with the hyperparameters defined in Table 1 below. Recall that N_l is the number of neurons in layer l , M_l is the number of samples of the signals created from the neurons of layer l , K_l is the kernel size of the neurons in layer l and D_l is the degree of the polynomials that need to be estimated for each neuron in layer l . Since the output layer is a single 1DCNN

Table 1: Hyperparameters for each layer of the networks used for the complexity estimation.

Hyperparameter	Layer		
	$l = 0$	$l = 1$	$l = 2$
M_l	100		
N_l	2	10	1
K_l		25	25
D_l		$\llbracket 1, 100 \rrbracket$	1

neuron, its execution time can be estimated separately from the first layer. That time will then be deducted from the overall execution time of the network. Subsequently, for each degree of polynomials in the previous set of hyperparameters, a 1DPNN is created, as well as its equivalent 1DCNN counterpart. 1000 forward propagations are first performed, then 1000 learning cycles (forward propagation and backpropagation) are performed. The execution times for 1 neuron are then estimated by deducting the average execution times of the last layer and then averaging over 1000 and dividing by N_1 .

The theoretical complexities determined in Eqs. (12) and (15) are expressed in terms of number of operations and need to be expressed in seconds. Therefore, given the execution times of the 1DPNN with $D_1 = 1$, we can estimate how long it would theoretically take to perform the same operations with a different polynomial degree. For instance, we can estimate the time T_1 it takes to perform a forward propagation as

a function of the polynomial degree D_1 using Eq. (12) as such:

$$\forall D_1 \in \llbracket 1, 100 \rrbracket, T_1(D_1) = D_1 T_0 + (D_1 - 1)(c_1 D_1 - c_2) T,$$

where:

- T_0 is the forward propagation execution time of a 1DCNN neuron,
- $c_1 = \frac{1}{2} M_0 N_0$,
- $c_2 = 2M_1$, and
- T is an estimate of the time it takes to perform one addition or one multiplication.

T can only be estimated from the fact that T_1 is an increasing function of D_1 which means that

$$\forall D_1 \in \llbracket 1, 100 \rrbracket, \frac{\partial T_1}{\partial D_1}(D_1) = T_0 + (2c_1 D_1 - (c_1 + c_2)) T \geq 0.$$

This is equivalent to:

$$\forall D_1 \in \llbracket 1, 100 \rrbracket, T \geq \frac{T_0}{c_1 + c_2 - 2c_1 D_1}.$$

Since $c_1 + c_2 - 2c_1 D_1$ is a decreasing function of D_1 , the final estimation of T is

$$T = \frac{T_0}{c_1 + c_2}.$$

The same can be done for the theoretical learning complexity defined in Eq. (15) by replacing c_1 , c_2 and T_0 accordingly.

4.2.3. Results

Figure 1 shows the evolution of the execution time of a neuron’s forward propagation with respect to the degree of the polynomial for each of the 1DCNN neuron, 1DPNN neuron and 1DPNN-equivalent neuron. Figure 1(a) also shows the evolution of the theoretical complexity with respect to the degree. This confirms that Eq. (12) is indeed an upper bound complexity and that, with optimization, the forward propagation of a 1DPNN neuron can run in quasi-linear time as shown in Figure 1(b). Moreover, with the chosen hyperparameters, the 1DPNN neuron is, on average, 1.94 times slower than the 1DPNN-equivalent neuron, which confirms the expectation that a 1DPNN neuron is more complex than a 1DPNN-equivalent neuron.

Figure 2 shows the evolution of the execution time of neuron’s learning process with respect to the degree of the polynomial for each of the 1DCNN neuron, 1DPNN neuron and 1DPNN-equivalent neuron. Figure 2(a) showing the evolution of the theoretical complexity with respect to the degree confirms that Eq. (15) is in fact an upper bound, and Figure 2(b) shows that the learning process of a 1DPNN neuron can also run in quasi-linear time, as stated in Section 3.4. However, the 1DPNN neuron’s learning process is, on average, 2.72 times slower than the 1DPNN-equivalent neuron, as it is to be expected from Eq. (15).

5. Experiments And Results

Since 1DPNN is basically an extension of 1DCNN, there is a need to compare the 1DPNN model’s performance with the 1DCNN model’s performance under certain conditions. In fact, the number of parameters in a 1DPNN differs from the number of parameters in a 1DCNN with the same topology, therefore we can devise 2 different comparison strategies that define the conditions of the experiments:

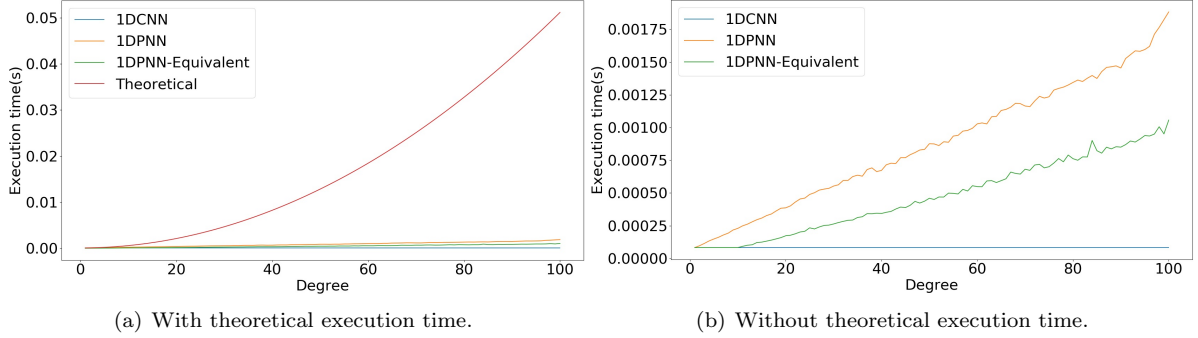


Figure 1: Forward propagation execution time for 1 neuron of each network.

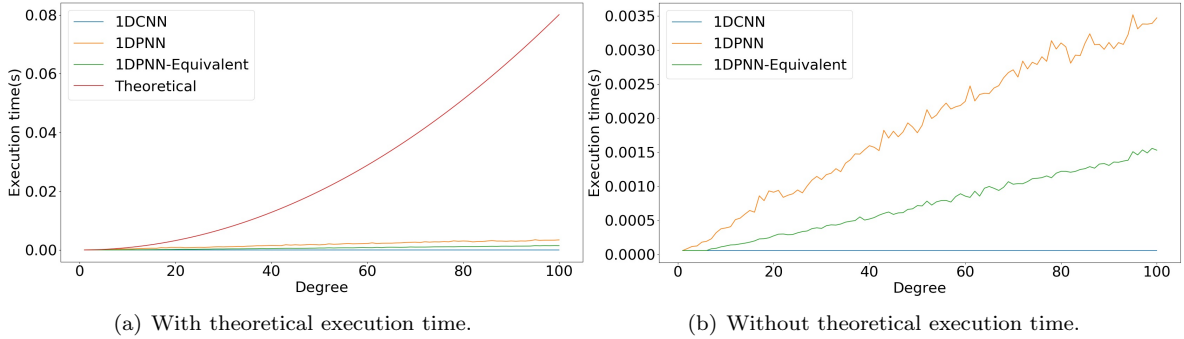


Figure 2: Learning process execution time for 1 neuron of each network.

1. **Topology-wise** comparison which consists in comparing the performances of a 1DCNN and a 1DPNN that both have the same topology.
2. **Parameter-wise** comparison which consist in comparing the performances of a 1DCNN and a 1DPNN that both have the same number of parameters. The 1DCNN is created according to the definition of the 1DPNN-equivalent network detailed in Section 4.2.

Both models will be evaluated on the same problems consisting of 2 classification problems which are musical note recognition on monophonic instrumental audio signals and spoken digit recognition and 2 regression problems which are audio signal denoising at 0db Signal-to-Noise Ratio (SNR) with Additive White Gaussian Noise (AWGN) and vocal source separation from a musical environment. The same learning rate will be used for all models on any given problem.

A comparison of the performances of both models on all the problems should be made by following the strategies described above. All problems involve 1 dimensional audio signals sampled at a given sampling rate and with a specific number of samples. However, the datasets used for the experiments contain either signals that have a high number of samples, or signals that have different numbers of samples inside the same dataset. Due to technical limitations, creating a network that takes a high number of samples as input or different number of samples per signal is time-consuming and irrelevant because the main aim of the experiments is to compare both models with each other, and not to produce state-of-the-art results on the considered problems. Therefore, the sliding window technique described below has been adopted for all the problems as a preprocessing step.

5.1. Sliding Window Technique

The sliding window technique consists on applying a sliding observation window on a signal to extract a

certain number of consecutive samples with a certain overlap between two consecutive windows. It is useful when dealing with signals that have a high number of samples and when studying a locally stationary signal property (such as the frequency of a tone which lasts for a certain duration).

Definition 4. Let $x = (x_0, \dots, x_{N-1}) \in \mathbb{R}^N$ be a temporal signal. Let $w \in \llbracket 1, N \rrbracket$ be the size of the window. Let $\alpha \in [0, 1[$ be the overlap ratio between two consecutive windows. We define $\mathcal{W}_{w,\alpha}(x)$ as the set of all the observed windows for the signal x , and we express it as such:

$$\mathcal{W}_{w,\alpha}(x) = \{(x_i, \dots, x_{i+w-1}) | i = \lfloor n(1-\alpha)w \rfloor, n \in \llbracket 0, \left\lfloor \frac{N-w}{(1-\alpha)w} \right\rfloor \rrbracket\}.$$

Remark 12. The sliding window has the effect of widening the spectrum of the signal due to the Heisenberg-Gabor uncertainty principle [39], thus, distorting it in a certain measure. Therefore, the size of the window has to be chosen so that a given observation window of the signal can contain enough information to process it accordingly.

5.2. Classification Problems

Since 1DPNN and 1DCNN are based on convolutions, they are basically used as regressors in the form of feature extractors. Their objective is to extract temporal features that will be used to classify the signals. In the case of this work, they are used to create a feature extractor block that will be linked to a classifier which will classify the input signals based on the features extracted as described in Figure 3, where x is a temporal signal, (f_1, \dots, f_p) are p features extracted using either 1DPNN or 1DCNN, and (c_1, \dots, c_q) are probabilities describing whether the signal x belongs to a certain class (there are q classes in general). The classifier will be a multilayer perceptron (MLP) in both problems and the metric used to evaluate the performance of the models is the classification accuracy. However, since the sliding window technique is used on all signals, the

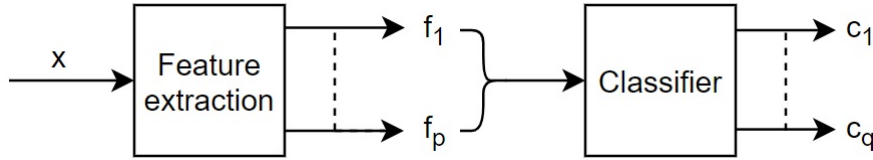


Figure 3: Block diagram of the classification procedure.

classifier will only be able to classify one window at a time. Therefore, for a given signal x , a window size w and an overlap ratio α as defined in the previous subsection, we end up with $|\mathcal{W}_{w,\alpha}(x)|$ different classes for the same signal, where $|\mathcal{W}_{w,\alpha}(x)|$ is the cardinal of $\mathcal{W}_{w,\alpha}(x)$. Thus, we define the class of the signal as the statistical mode of all the classes estimated from every window extracted from the signal. For instance, if we have 3 classes and a signal gets decomposed in 10 windows such that 5 windows are classified as class 0, 2 windows as class 1, and 3 windows as class 2, the signal will be classified as class 0 since it is the class that is represented the most in the estimated classes. As a result, the performance of each model is evaluated with respect to the per-window accuracy and the per-signal accuracy.

5.2.1. Note Recognition on Monophonic Instrumental Audio Signals

The dataset used for this problem is NSynth [17] which is a large scale dataset of annotated musical notes produced by various instruments. It contains more than 300,000 signals sampled at 16kHz, and lasting 4 seconds each. The usual musical range is composed of 88 different notes which represent our classes. Since the dataset is huge, we only use 12,678 signals for training, and 4096 for testing. We also use a sliding window with a window size $w = 1600$ and an overlap of 0.5 which makes the training set composed of 728,828 signals and the test set composed of 235,480 signals. We then use 10-fold cross validation [40] on

the training set so that we estimate the average performance for every topology used on the test set.

Three different networks were created, a network composed of a 1DPNN feature extractor, a network composed of a 1DCNN feature extractor with the same topology as the previous one, and a network composed of a 1DCNN feature extractor with the same number of parameters as the 1DPNN. Table 2 shows the hyperparameters of each layer of the 1DPNN, and the last network. These networks are trained on the

Table 2: Networks' topologies for note recognition.

1DPNN	1DPNN-equivalent network
PNNLayer(neurons=12, kernel=441, degree=2, activation='relu')	Conv1D(neurons=12, kernel=441, activation='relu')
MaxPooling1D(2)	Conv1D(neurons=12, kernel=221, activation='relu')
PNNLayer(neurons=12, kernel=221, degree=2, activation='relu')	Conv1D(neurons=12, kernel=111, activation='relu')
MaxPooling1D(2)	MaxPooling1D(2)
PNNLayer(neurons=12, kernel=81, degree=2, activation='relu')	Conv1D(neurons=12, kernel=81, activation='relu')
MaxPooling1D(2)	MaxPooling1D(2)
PNNLayer(neurons=12, kernel=49, degree=2, activation='relu')	Conv1D(neurons=12, kernel=49, activation='relu')
MaxPooling1D(2)	MaxPooling1D(2)
Flatten	Flatten
MLP(neurons=64, activation='relu')	MLP(neurons=64, activation='relu')
MLP(neurons=88, activation='softmax')	MLP(neurons=88, activation='softmax')

windows extracted from the signals, and their average accuracy with 10-fold cross validation is reported in Table 3 below in percentages. We can see that the average accuracy per window of the 1DPNN is slightly better than the other networks. Figure 4 also shows that 94% of the time, over 100 epochs, the average

Table 3: Accuracy per window for each network for note recognition over 10 folds.

Statistic (%)	Network		
	1DPNN	1DCNN same topology	1DPNN-equivalent
Minimum accuracy	79.9	75.3	77
Maximum accuracy	81.1	78	80.2
Average accuracy	80	77	79.47

accuracy of the 1DPNN is higher than the 1DPNN-equivalent network.

The networks are evaluated on whether they can classify a window from a signal correctly, but they should be evaluated on whether they classify a complete signal since the dataset is originally composed of 4 second signals. In the case of this work, multiple windows are derived from a single signal that belongs to a certain class. Therefore, the windows are also considered as belonging to the same class of the signal that they are derived from. However, the models may give a different classification for each window, so to determine the class of a signal given the classification of its windows, we use the statistical mode of the different classifications. By performing this postprocessing step, we end up with the average accuracy per signal for each network, as shown in Table 4. We notice that the per-signal accuracies are better than the per-window accuracies for all networks, and that the 1DPNN is 5% better at classifying the signals than the 1DCNN with the same number of parameters.

5.2.2. Spoken Digit Recognition

The dataset used for this problem is the Free Spoken Digits Dataset [18] which contains 2000 audio

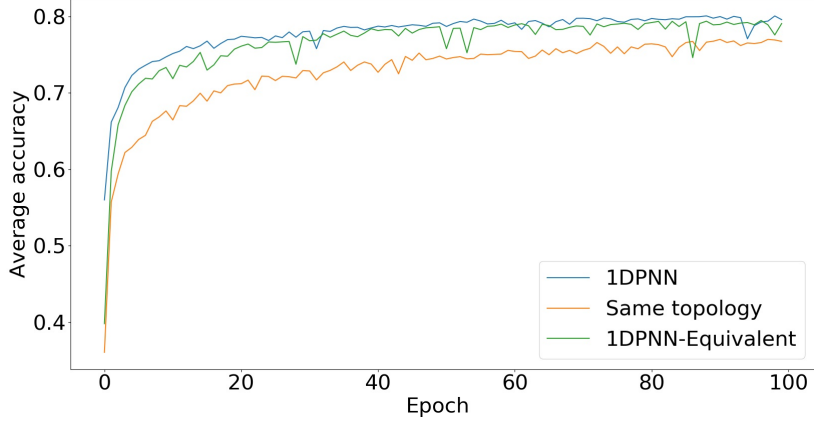


Figure 4: Average accuracy for each epoch of all the networks trained on the note recognition dataset.

Table 4: Accuracy per signal for each network for note recognition over 10 folds.

Statistic (%)	Network		
	1DPNN	1DCNN same topology	1DPNN-equivalent
Average accuracy	86.6	79.3	81.7

signals of different duration sampled at 8kHz consisting of people uttering digits from 0 to 9 which will represent the classes of the signals. In this work 1800 signals will be considered for training and 200 signals will be considered for testing the networks. Since the dataset has signals of different durations, we use a sliding window with a window size of $w = 1600$ and an overlap of 0.5 which makes the training set composed of 4538 signals and the test set composed of 504 signals. 10-fold cross validation is also used to evaluate the three networks. Table 5 shows the hyperparameters of each layer of the 1DPNN and the 1DPNN-equivalent

Table 5: Networks' topologies for spoken digit recognition.

1DPNN	1DPNN-equivalent network
PNNLayer(neurons=12, kernel=81, degree=1, activation='tanh')	Conv1D(neurons=24, kernel=81, activation='tanh')
MaxPooling1D(2)	Conv1D(neurons=24, kernel=25, activation='tanh')
PNNLayer(neurons=12, kernel=25, degree=3, activation='tanh')	MaxPooling1D(2)
MaxPooling1D(2)	Conv1D(neurons=16, kernel=25, activation='tanh')
PNNLayer(neurons=12, kernel=9, degree=5, activation='tanh')	MaxPooling1D(2)
MaxPooling1D(2)	Conv1D(neurons=12, kernel=9, activation='tanh')
PNNLayer(neurons=12, kernel=9, degree=7, activation='tanh')	MaxPooling1D(2)
MaxPooling1D(2)	Conv1D(neurons=12, kernel=9, activation='tanh')
Flatten	MaxPooling1D(2)
MLP(neurons=64, activation='relu')	Flatten
MLP(neurons=48, activation='relu')	MLP(neurons=64, activation='relu')
MLP(neurons=10, activation='softmax')	MLP(neurons=48, activation='relu')
	MLP(neurons=10, activation='softmax')

network.

The 10-fold accuracy statistics of each network is shown in Table 6 where the average accuracy of the 1DPNN is almost 3% better than the 1DPNN-equivalent network. Figure 5 shows that over 200 epochs, 84% of the time, the average accuracy of the 1DPNN is higher than that of the 1DPNN-equivalent network. Since the classification is performed window-wise, the average accuracy per signal can be estimated with the same principle used in the note recognition problem. Table 7 shows that the average accuracy per signal of the 1DPNN surpasses that of the 1DPNN-equivalent network by 5.3%.

Table 6: Accuracy per window for each network for spoken digit recognition over 10 folds.

Statistic (%)	Network		
	1DPNN	1DCNN same topology	1DPNN-equivalent
Minimum accuracy	79.17	73.74	77.86
Maximum accuracy	82.21	76.93	79.61
Average accuracy	81.07	75.29	78.48

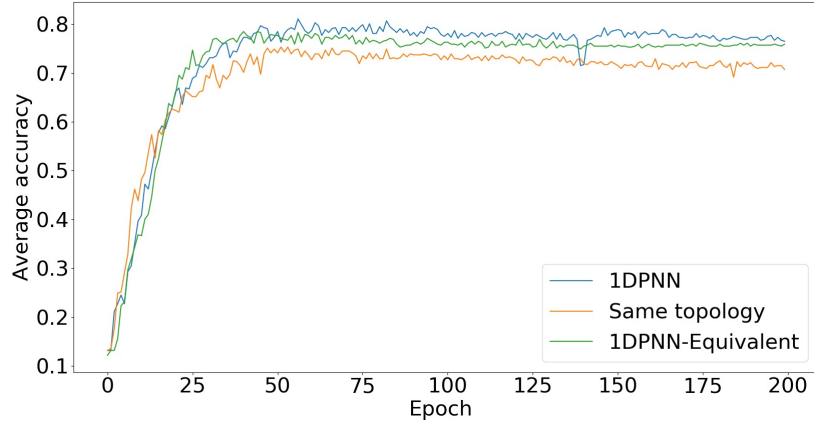


Figure 5: Average accuracy for each epoch of all the networks trained on the spoken digit recognition dataset.

Table 7: Accuracy per signal for each network for spoken digit recognition over 10 folds.

Statistic (%)	Network		
	1DPNN	1DCNN same topology	1DPNN-equivalent
Average accuracy	86.22	78.57	80.9

5.3. Regression Problems

Both 1DPNN and 1DCNN models take as input a signal and output a signal that usually has a lower temporal dimension due to border effects. However, in both regression problems that are considered, we need the output signal to have the same temporal dimension as the input signal. Therefore, we use zero-padding to avoid border effects. The metric that is used to evaluate the performances of the models for both problems is the Signal-to-Noise Ratio (SNR) measured in decibel (dB) defined as such:

$$SNR = 10 \log_{10} \left(\frac{\mu_{s^2}}{\mu_{n^2}} \right),$$

where μ_{s^2} is the mean square of the signal without noise, and μ_{n^2} is the mean square of the noise. The dataset used for both problems is the MUSDB18 [19] dataset containing 150 high quality full length stereo musical tracks (10 hours of recordings) with their isolated drums, bass, and vocal stems sampled at 44.1kHz. It is mainly used for source separation, but can also be used for instrument tracking or for noise reduction.

5.3.1. Audio Signal Denoising

The aim of this problem is to restore voice recordings that are drowned in AWGN making their individual SNR around 0dB. However, since the dataset is huge and the experiments are restricted by technical limitations, we take a small subset of the training set and the test set, downsample the voice tracks to 16kHz, and extract windows of 100ms to obtain 40,000 short clips (80% for training, 20% for testing). The topologies used to solve the problem are detailed in Table 8 below. The statistics on the SNR gathered using 10-fold cross validation are reported in Table 9 where we notice that the 1DPNN is slightly better than the 1DPNN-equivalent. However, Figure 6 representing the evolution of the 10-fold average SNR over the epochs shows that the 1DPNN has a highly faster convergence than the other networks.

Table 8: Networks' topologies for audio signal denoising.

1DPNN	1DPNN-equivalent network
PNNLayer(neurons=12, kernel=371, degree=6, activation='tanh')	Conv1D(neurons=38, kernel=371, activation='tanh')
MaxPooling1D(2)	MaxPooling1D(2)
PNNLayer(neurons=12, kernel=49, degree=8, activation='tanh')	Conv1D(neurons=38, kernel=49, activation='tanh')
UpSampling1D(2)	UpSampling1D(2)
PNNLayer(neurons=1, kernel=27, degree=9, activation='tanh')	Conv1D(neurons=1, kernel=27, activation='tanh')

Table 9: SNR statistics for each network for audio signal denoising over 10 folds.

Statistic (dB)	Network		
	1DPNN	1DCNN same topology	1DPNN-equivalent
Minimum SNR	6.28	5.53	6.23
Maximum SNR	6.42	6.07	6.35
Average SNR	6.34	5.88	6.31

5.3.2. Vocal Source Separation

The aim of this problem is to extract the vocal source from a musical recording containing musical instruments such as drums or bass. Since all signals in the dataset are stereo signals and sampled at 44.1kHz, it is very much time-consuming to produce fully trained models on the entire dataset. Due to technical limitations, we take a small subset of the training set and the test set, extract windows of 200ms to obtain 150,000 short clips (120,000 for training and 30,000 for testing). The topologies used to solve the problem are detailed in Table 10 below. The statistics on the SNR gathered using 10-fold cross validation are reported in Table 11 where we notice that there is a clear gap showing that even the worst 1DPNN performed better than the best 1DPNN-equivalent network. Figure 7 further emphasizes this gap by showing the 10-fold average SNR over 100 epochs. It also shows that after only 10 epochs, the 1DPNN model starts to exceed the best average SNR achieved by the 1DCNN model in 100 epochs.

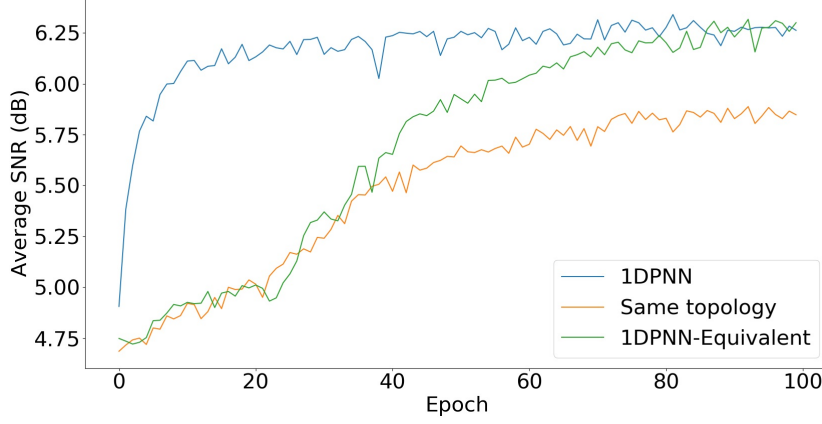


Figure 6: Average SNR in dB for each epoch of all the networks trained on audio signal denoising.

Table 10: Networks' topologies for vocal source separation.

1DPNN	1DPNN-equivalent Network
PNNLayer(neurons=12, kernel=81, degree=2, activation='tanh')	Conv1D(neurons=16, kernel=81, activation='tanh')
PNNLayer(neurons=12, kernel=2, degree=2, activation='tanh', strides=2)	Conv1D(neurons=16, kernel=2, activation='tanh', strides=2)
PNNLayer(neurons=12, kernel=49, degree=2, activation='tanh')	Conv1D(neurons=16, kernel=49, activation='tanh')
PNNLayer(neurons=12, kernel=2, degree=2, activation='tanh', strides=2)	Conv1D(neurons=16, kernel=2, activation='tanh', strides=2)
PNNLayer(neurons=12, kernel=25, degree=2, activation='tanh')	Conv1D(neurons=19, kernel=25, activation='tanh')
UpSampling1D(2)	UpSampling1D(2)
PNNLayer(neurons=12, kernel=49, degree=2, activation='tanh')	Conv1D(neurons=19, kernel=49, activation='tanh')
UpSampling1D(2)	UpSampling1D(2)
PNNLayer(neurons=2, kernel=25, degree=2, activation='tanh')	Conv1D(neurons=2, kernel=25, activation='tanh')

Table 11: SNR statistics for each network for vocal source separation over 10 folds.

Statistic (dB)	Network		
	1DPNN	1DCNN same topology	1DPNN-equivalent
Minimum SNR	1.93	1.61	1.76
Maximum SNR	2.31	1.82	1.91
Average SNR	2.08	1.73	1.81

6. Conclusion

In this paper, we have formally introduced a novel 1-Dimensional Polynomial Neural Network (1DPNN) model that induces a high degree of non-linearity starting from the initial layer in an effort to produce compact topologies in the context of audio signal applications. Our experiments demonstrate it has the potential to produce more accurate feature extraction and better regression than the conventional 1DCNN.

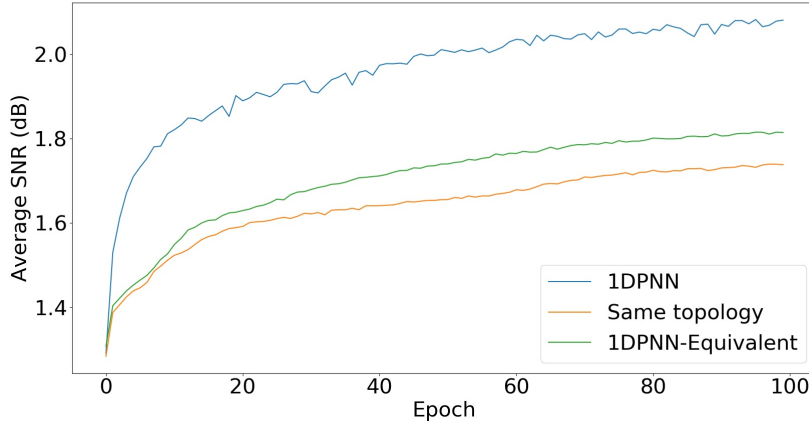


Figure 7: Average SNR in dB for each epoch of all the networks trained on vocal source separation.

Furthermore, our model also shows faster convergence in audio signal denoising and vocal source separation problems. We have also demonstrated that the 1DPNN model converges when we use activation functions bounded between -1 and 1 or when all the degrees are set to 1 because it becomes equivalent to a 1DCNN.

Our experiments are not sufficient to claim that our proposed 1DPNN surpasses 1DCNN on all class of complex classification and regression problems. In addition, there is still no mathematical proof that the 1DPNN is a convergent model. Moreover, the choice of the degree of every layer of the networks created for the experiments was specifically designed to evaluate the performances. Therefore, a method that accurately estimates the appropriate degree for each layer needs to be created in order to replace the manual hyperparameter search. Furthermore, the stability of the model is not ensured as stacked layers with high degrees can lead to the model becoming unstable, thus, losing its generalization capability. Therefore, there is also a need to estimate an upper bound limit for the degree of each layer so that the overall network stably learns from the given data. Finally, due to computational limits, the model could not be tested with deep topologies that are used to solve very complex classification and regression problems involving a huge amount of data.

Future work may be done on demonstrating the conditions of the stability of the model as well as its convergence. Furthermore, a method that automatically sets the degree of each 1DPNN layer depending on the problem tackled may be developed as to provide further independence from manual search. Moreover, the equations defining the 1DPNN model and its backpropagation can easily be extended to 2 dimensions and to 3 dimensions, thus, providing new models to deal with image processing and video processing problems for example. In addition, a more specific gradient descent optimization scheme may be developed to avoid gradient explosion. Finally, deeper 1DPNN topologies can be created to compete with state-of-the-art models on any 1 dimensional signal related problem, not only audio signals. More thorough experiments and further mathematical analysis can help this model to thrive and find its place as a standard model in the deep learning field.

Acknowledgement

This work was funded by the Mitacs Globalink Graduate Fellowship Program (no. FR41237) and the NSERC Discovery Grants Program (nos. 194376, 418413).

References

- [1] J. Schmidhuber, "Deep learning in neural networks: An overview," *Neural Networks*, vol. 61, pp. 85 – 117, 2015. <https://doi.org/10.1016/j.neunet.2014.09.003>.

- [2] Y. LeCun, P. Haffner, L. Bottou, and Y. Bengio, "Object recognition with gradient-based learning," in *Shape, Contour and Grouping in Computer Vision*, (Berlin, Heidelberg), p. 319, Springer-Verlag, 1999.
- [3] K. Fukushima, "Neocognitron: A self-organizing neural network model for a mechanism of pattern recognition unaffected by shift in position," *Biol. Cybernetics*, vol. 36, p. 193202, 1980. <https://doi.org/10.1007/BF00344251>.
- [4] Pearlmutter, "Learning state space trajectories in recurrent neural networks," in *International 1989 Joint Conference on Neural Networks*, pp. 365–372 vol.2, 1989. <https://doi.org/10.1109/IJCNN.1989.118724>.
- [5] A. Cleeremans, D. Servan-Schreiber, and J. L. McClelland, "Finite state automata and simple recurrent networks," *Neural Computation*, vol. 1, no. 3, pp. 372–381, 1989. <https://doi.org/10.1162/neco.1989.1.3.372>.
- [6] S. Liu and W. Deng, "Very deep convolutional neural network based image classification using small training sample size," in *2015 3rd IAPR Asian Conference on Pattern Recognition (ACPR)*, pp. 730–734, 2015. <https://doi.org/10.1109/ACPR.2015.7486599>.
- [7] J. Salamon and J. P. Bello, "Deep convolutional neural networks and data augmentation for environmental sound classification," *IEEE Signal Processing Letters*, vol. 24, no. 3, pp. 279–283, 2017. <https://doi.org/10.1109/LSP.2017.2657381>.
- [8] S. Oeda, I. Kurimoto, and T. Ichimura, "Time series data classification using recurrent neural network with ensemble learning," in *Knowledge-Based Intelligent Information and Engineering Systems* (B. Gabrys, R. J. Howlett, and L. C. Jain, eds.), (Berlin, Heidelberg), pp. 742–748, Springer Berlin Heidelberg, 2006.
- [9] Z. Che, S. Purushotham, K. Cho, D. Sontag, and Y. Liu, "Recurrent neural networks for multivariate time series with missing values," *Scientific Reports*, vol. 8, p. 6085, Apr 2018. <https://doi.org/10.1038/s41598-018-24271-9>.
- [10] A. Krizhevsky, I. Sutskever, and G. E. Hinton, "Imagenet classification with deep convolutional neural networks," in *Advances in Neural Information Processing Systems 25* (F. Pereira, C. J. C. Burges, L. Bottou, and K. Q. Weinberger, eds.), pp. 1097–1105, Curran Associates, Inc., 2012.
- [11] C. Szegedy, Wei Liu, Yangqing Jia, P. Sermanet, S. Reed, D. Anguelov, D. Erhan, V. Vanhoucke, and A. Rabinovich, "Going deeper with convolutions," in *2015 IEEE Conference on Computer Vision and Pattern Recognition (CVPR)*, pp. 1–9, 2015.
- [12] K. Hornik, M. Stinchcombe, and H. White, "Multilayer feedforward networks are universal approximators," *Neural Networks*, vol. 2, no. 5, pp. 359 – 366, 1989. [https://doi.org/10.1016/0893-6080\(89\)90020-8](https://doi.org/10.1016/0893-6080(89)90020-8).
- [13] T. Hofmann, B. Schölkopf, and A. J. Smola, "Kernel methods in machine learning," *Ann. Statist.*, vol. 36, pp. 1171–1220, 06 2008. <https://doi.org/10.1214/009053607000000677>.
- [14] Y. Cho and L. K. Saul, "Kernel methods for deep learning," in *Advances in Neural Information Processing Systems 22* (Y. Bengio, D. Schuurmans, J. D. Lafferty, C. K. I. Williams, and A. Culotta, eds.), pp. 342–350, Curran Associates, Inc., 2009.
- [15] J. Mairal, P. Koniusz, Z. Harchaoui, and C. Schmid, "Convolutional kernel networks," in *Advances in Neural Information Processing Systems 27* (Z. Ghahramani, M. Welling, C. Cortes, N. D. Lawrence, and K. Q. Weinberger, eds.), pp. 2627–2635, Curran Associates, Inc., 2014.
- [16] D. Chen, L. Jacob, and J. Mairal, "Recurrent kernel networks," in *Advances in Neural Information Processing Systems 32* (H. Wallach, H. Larochelle, A. Beygelzimer, F. d'Alché Buc, E. Fox, and R. Garnett, eds.), pp. 13431–13442, Curran Associates, Inc., 2019.
- [17] J. Engel, C. Resnick, A. Roberts, S. Dieleman, M. Norouzi, D. Eck, and K. Simonyan, "Neural audio synthesis of musical notes with wavenet autoencoders," in *Proceedings of the 34th International Conference on Machine Learning - Volume 70*, ICML17, p. 10681077, JMLR.org, 2017.
- [18] [dataset] Zohar Jackson, C. Souza, J. Flaks, and H. Nicolas, "Jakobovski/free-spoken-digit-dataset v1.0.6," Oct. 2017. <https://doi.org/10.5281/zenodo.1039893>.
- [19] [dataset] Z. Rafii, A. Liutkus, F.-R. Stöter, S. I. Mimilakis, and R. Bittner, "The MUSDB18 corpus for music separation," Dec. 2017. <https://doi.org/10.5281/zenodo.1117372>.
- [20] B. Graham, "Fractional max-pooling," *CoRR*, vol. abs/1412.6071, 2014.
- [21] C.-Y. Lee, P. W. Gallagher, and Z. Tu, "Generalizing pooling functions in convolutional neural networks: Mixed, gated, and tree," in *Proceedings of the 19th International Conference on Artificial Intelligence and Statistics* (A. Gretton and C. C. Robert, eds.), vol. 51 of *Proceedings of Machine Learning Research*, (Cadiz, Spain), pp. 464–472, PMLR, 09–11 May 2016.
- [22] N. Srivastava, G. Hinton, A. Krizhevsky, I. Sutskever, and R. Salakhutdinov, "Dropout: A simple way to prevent neural networks from overfitting," *J. Mach. Learn. Res.*, vol. 15, p. 19291958, Jan. 2014.
- [23] S. Ioffe and C. Szegedy, "Batch normalization: Accelerating deep network training by reducing internal covariate shift," in *Proceedings of the 32nd International Conference on International Conference on Machine Learning - Volume 37*, ICML'15, p. 448456, JMLR.org, 2015.
- [24] A. F. Agarap, "Deep learning using rectified linear units (relu)," *CoRR*, vol. abs/1803.08375, 2018.
- [25] J. Turian, J. Bergstra, and Y. Bengio, "Quadratic features and deep architectures for chunking," in *Proceedings of Human Language Technologies: The 2009 Annual Conference of the North American Chapter of the Association for Computational Linguistics, Companion Volume: Short Papers*, (Boulder, Colorado), pp. 245–248, Association for Computational Linguistics, June 2009.
- [26] R. Livni, S. Shalev-Shwartz, and O. Shamir, "A provably efficient algorithm for training deep networks," *CoRR*, vol. abs/1304.7045, 2013.
- [27] C. Wang, J. Yang, L. Xie, and J. Yuan, "Kervolutional neural networks," in *2019 IEEE/CVF Conference on Computer Vision and Pattern Recognition (CVPR)*, pp. 31–40, 2019. <https://doi.org/10.1109/CVPR.2019.00012>.
- [28] K. He, X. Zhang, S. Ren, and J. Sun, "Deep residual learning for image recognition," in *2016 IEEE Conference on Computer Vision and Pattern Recognition (CVPR)*, pp. 770–778, 2016. <https://doi.org/10.1109/CVPR.2016.90>.

- [29] J. Mairal, “End-to-end kernel learning with supervised convolutional kernel networks,” in *Advances in Neural Information Processing Systems 29* (D. D. Lee, M. Sugiyama, U. V. Luxburg, I. Guyon, and R. Garnett, eds.), pp. 1399–1407, Curran Associates, Inc., 2016.
- [30] N. Aronszajn, “Theory of reproducing kernels,” *Trans. Amer. Math. Soc.*, vol. 68, pp. 337–404, 1950.
- [31] C. Dong, C. C. Loy, K. He, and X. Tang, “Learning a deep convolutional network for image super-resolution,” in *Computer Vision – ECCV 2014* (D. Fleet, T. Pajdla, B. Schiele, and T. Tuytelaars, eds.), (Cham), pp. 184–199, Springer International Publishing, 2014.
- [32] D. T. Tran, S. Kiranyaz, M. Gabbouj, and A. Iosifidis, “Heterogeneous multilayer generalized operational perceptron,” *IEEE Transactions on Neural Networks and Learning Systems*, vol. 31, no. 3, pp. 710–724, 2020. <https://doi.org/10.1109/TNNLS.2019.2914082>.
- [33] S. Kiranyaz, T. Ince, A. Iosifidis, and M. Gabbouj, “Operational neural networks,” *Neural Computing and Applications*, vol. 32, p. 66456668, 2020.
- [34] S. Kiranyaz, J. Malik, H. Ben Abdallah, T. Ince, A. Iosifidis, and M. Gabbouj, “Self-organized operational neural networks with generative neurons,” *CoRR*, vol. abs/2004.11778, 2020.
- [35] A. CAUCHY, “Methode generale pour la resolution des systemes d’equations simultanees,” *C.R. Acad. Sci. Paris*, vol. 25, pp. 536–538, 1847.
- [36] X. Glorot and Y. Bengio, “Understanding the difficulty of training deep feedforward neural networks,” in *Proceedings of the Thirteenth International Conference on Artificial Intelligence and Statistics* (Y. W. Teh and M. Titterton, eds.), vol. 9 of *Proceedings of Machine Learning Research*, (Chia Laguna Resort, Sardinia, Italy), pp. 249–256, PMLR, 13–15 May 2010.
- [37] M. Abadi, A. Agarwal, P. Barham, E. Brevdo, Z. Chen, C. Citro, G. S. Corrado, A. Davis, J. Dean, M. Devin, S. Ghemawat, I. Goodfellow, A. Harp, G. Irving, M. Isard, Y. Jia, R. Jozefowicz, L. Kaiser, M. Kudlur, J. Levenberg, D. Mané, R. Monga, S. Moore, D. Murray, C. Olah, M. Schuster, J. Shlens, B. Steiner, I. Sutskever, K. Talwar, P. Tucker, V. Vanhoucke, V. Vasudevan, F. Viégas, O. Vinyals, P. Warden, M. Wattenberg, M. Wicke, Y. Yu, and X. Zheng, “TensorFlow: Large-scale machine learning on heterogeneous systems.” <https://www.tensorflow.org/>, 2015. (accessed 27 July 2020).
- [38] F. Chollet *et al.*, “Keras.” <https://github.com/fchollet/keras>, 2015. (accessed 27 July 2020).
- [39] D. Gabor, “Theory of communication. part 1: The analysis of information,” *Journal of the Institution of Electrical Engineers - Part III: Radio and Communication Engineering*, vol. 93, no. 26, pp. 429–441, 1946. <https://doi.org/10.1049/ji-3-2.1946.0074>.
- [40] P. Refaellizadeh, L. Tang, and H. Liu, *Cross-Validation*, pp. 532–538. Boston, MA: Springer US, 2009. https://doi.org/10.1007/978-0-387-39940-9_565.